Supplementary Information File for

An expedient bone tool used for flaying carcasses by Neanderthal at the Abri du Maras (France)

Luc Doyon[1*], Juan Marín Hernando[2,3,4], Marie-Hélène Moncel[3],
Maïlys Richard[5,6], Francesco d'Errico[1,7]

[1] Université de Bordeaux, UMR5199 PACEA, CNRS, MCC; Pessac, 33615, France.
[2] Department of Prehistory and Archaeology, Universidad Nacional de Educación a Distancia, UNED; Madrid, 28040, Spain.
[3] UMR 7194-CNRS-MNHN, Institut de Paléontologie Humaine; Paris, 75013, France.
[4] Institut Català de Paleoecologia Humana i Evolució Social – IPHES; Tarragona, 43007, Spain
[5] Archéosciences Bordeaux, UMR 6034 CNRS, Université Bordeaux Montaigne ; Pessac, 33607, France
[6] Department of Early Prehistory and Quaternary Ecology, University of Tübingen; Tübingen, 72070, Germany
[7] University of Bergen, Centre for Early Sapiens Behaviour (SapienCE), Department of Archaeology, History, Cultural Studies and Religion; Bergen, 5020, Norway
*Corresponding author. Email: luc.doyon@u-bordeaux.fr.

The PDF file includes:

Supplementary Text S1 to S3

Supplementary Figs. S1 to S8

Supplementary Tables S1 to S10

Other Supplementary Materials for this manuscript include the following:

Supplementary Data S1

Supplementary Text

Supplementary Text S1. Surface texture data file structure

The surface texture data file includes seven categorical columns and 41 columns for the quantitative parameters extracted during the post-acquisition processing phase of the analysis. The file must be saved in *.csv format

Categorical variables

- Acquisition_ID: unique identifier which, in the present study, corresponds to the concatenated text of the Acquisition name and the Extracted zone (A, B, C, D, or E). Spaces are replaced by underscores.
- Name: name of the acquisition.
- Zone: letter identifying the extracted zone
- Spec: distinguishes between archaeological (A) or experimental (E) specimens.
- CAT: refers to the type of surface, either used (Used) or altered by taphonomic processes (Tapho) on the archaeological specimens, or used in an experimental setting (Exper) for the experimental replica.
- Region: corresponds to the nature of the analysed surface and can be either cortical (Cort), medullar (Medu) or the fracture plane (Frac).
- Concat: is a concatenation of the first letter of CAT and the Region separated with an underscore.
- Lev1: refers to the first level of worked material in the ExOsTechBank, which captures the broad categories that can usually be inferred with high accuracy using traditional use wear methods.
- Lev2: refers to the second level of worked material in the ExOsTechBank, which captures in more detail the specific nature of the activity, the state of the worked material and the use of abrasives in the task.

For the categorical variables, the use of numerical values should be avoided. Columns with numerical values should only be restricted the surface texture parameters.

Surface roughness parameters

By default, the values for 43 surface roughness parameters are extracted for each sub-area of each acquisition. Their abbreviated codes, descriptions and units are presented in Supplementary Table S1.

Supplementary Text S2. Quantitative surface texture analysis workflow

It is assumed that the *.csv data file and the R script is saved in the same directory which is set as the "Working Directory" in the R environment. No script is provided for this.

Step 0: saves several external functions in the environment to facilitate the transformation and integration of non-linear variables in multivariate analyses.

Step 1: imports the data file in R, creates the output directory, eliminates column with null values, creates separate data frames for the archaeological and experimental specimens, and defines the column with angle and percentage/ratio values.

Step 2: computes a primary exploration of the data on the archaeological acquisition. Two functions are included in this step, one dealing with linear variables (A) and one for circular data (B). It automatically generates boxplots – or rose diagrams for circular variables – and statistical tests for each roughness variables. The normality of the distributions is first tested to establish the best statistical approach to proceed with pairwise comparisons. Then, the appropriate test is performed, and the results are saved in a summary table. Plots are saved with significant pairs being indicated on them. This step is meant to compare first and

foremost whether significant differences in surface texture are observed between taphonomically altered surfaces and those interpreted as bearing use wear pattern.

Step 3: filters the surface texture parameters to be included in multivariate analyses. To perform this task, variables that yielded significant results in summary table generated in Step 2 are first selected, and then, highly correlated variables among them are removed keeping only one variable for each correlated pair. The significant and highly correlated variables are listed and tables limited to filtered data are produced. The non-numerical metadata is appended to the filtered data and, if needed, data is transformed for the variables expressed in angles, percentages or ratio. A correlation matrix combining the pairwise comparison between linear, and circular variables is also generated.

Step 4: computes a PCA for the various surfaces from the archaeological specimen. Confidence threshold for the ellipse, start and end columns with numeric data to be used in the PCA, and PC dimensions should be updated before running the script.

Step 5: computes an LDA with the surface texture data and a cross-validation CVA with the PCA data to assess to what degree it is possible to discriminate between the worn and unworn surfaces (group_column) on the archaeological specimen by the type of surface (supra). The training set uses 80% of the sample and the testing set uses the remaining data. *Note*: if only two categories are used as group_column within a region, the results are displayed as histogram with superimposed density curves, otherwise, they are displayed with scatterplots and ellipses of confidence.

As of that step, the results should be reassessed to establish whether new acquisitions are needed, e.g., if the one made didn't capture true use wear in comparison with other taphonomically altered surfaces, or if it should be simply discarded because worn and unworn areas cannot be discriminated from one another. This assessment should rely mainly on the overall and class statistics computed in Step 5.

Step 6: computes a primary exploration of the data for the experimental acquisition. Two functions are included in this step, one dealing with linear variables (A) and one for circular data (B). It automatically generates boxplots – or rose diagrams for circular variables – and statistical tests for each roughness variables. The normality of the distributions is first tested to establish the best statistical approach to proceed with pairwise comparisons. Then, the appropriate test is performed, and the results are saved in a summary table. Plots are saved with significant pairs being indicated on them. This step is meant to compare first and foremost whether significant differences in surface texture are observed between use wear pattern generated in different activities. As such, it focuses on "Lev1", which captures the broad categories that can usually be inferred with high accuracy using traditional use wear methods.

Step 7: filters the surface texture parameters to be included in multivariate analyses. To perform this task, variables that yielded significant results in summary table generated in Step 6 are first selected, and then, highly correlated variables among them are removed keeping only one variable for each correlated pair. The significant and highly correlated variables are listed and tables limited to filtered data are produced. The non-numerical metadata is appended to the filtered data and, if needed, data is transformed for the variables expressed in angles, percentages or ratio. A correlation matrix combining the pairwise comparison between linear, and circular variables is also generated. This is essentially a repeat of Step 2 but based on the experimental results. It, however, filters the variables directly from the table produced after eliminating null data in Step 1.

Step 8: computes a PCA for the various surfaces from the experimental sample and includes the acquisitions on the archaeological specimen as supplementary individuals, i.e.,

individuals that are transformed without adding weight to the PCA. Confidence threshold for the ellipse and PC dimensions should be updated each time before running the script.

Step 9: removes outliers identified in the PCA and filters the experimental and archaeological acquisitions to retain only those made on the cortical surface of bone. This latter process is temporarily added owing to the nature of the data comprised in the ExOsTechBank. With further acquisitions, i.e., when the sample size for those made on cortical and medullar surfaces as well as fracture planes becomes more balanced across experiments, it could be discarded while retaining the function to deal with outliers. Outliers are listed and removed from the filtered data (Step 7) and from the PCA results (Step 8).

Step 10: computes an LDA with the surface texture data and a cross-validation CVA with the PCA data to assess to what degree it is possible to discriminate between the worn surfaces assigned to distinct "Lev1" categories in the experimental sample. To avoid sample imbalance, the minimal number of acquisitions for any "Lev1" category is established. The training set uses a random selection of 80% of that minimal number for all "Lev1" categories included in the experimental sample. The testing set uses the remaining experimental data. After generating the LDA and cross-validation CVA as well as predicting the "Lev1" class for the testing set with both approaches, the model's accuracy statistics are saved. The process, i.e., from the selection of the training set to the calculation of the models' accuracy statistics, is repeated 1001 times. Following the iterations, the model that performed best is used to predict the "Lev1" class for the archaeological acquisitions. Histograms of the distribution for the accuracy percentage and the kappa statistics across the iterations are produced as well as tables with the best model statistics, the LD/CV coefficient from the best model, and a summary of the iteration results. *Note*: if only two categories are used as group_column within a region, the results are displayed as histogram with superimposed density curves, otherwise, they are displayed with scatterplots and ellipses of confidence.

Step 11: extracts the two "Lev1" class that were most often predicted for the archaeological acquisitions. It then computes an LDA with the surface texture data and a cross-validation CVA with the PCA data to assess to what degree it is possible to discriminate between the worn surfaces assigned to distinct "Lev2" categories in the experimental sample. To avoid sample imbalance, the minimal number of acquisitions for any "Lev2" category is established. The training set uses a random selection of 80% of that minimal number for all "Lev2" categories included in the experimental sample. The testing set uses the remaining experimental data. After generating the LDA and cross-validation CVA as well as predicting the "Lev2" class for the testing set with both approaches, the model's accuracy statistics are saved. The process, i.e., from the selection of the training set to the calculation of the models' accuracy statistics, is repeated 1001 times. Following the iterations, the model that performed best is used to predict the "Lev2" class for the archaeological acquisitions. Histograms of the distribution for the accuracy percentage and the kappa statistics across the iterations are produced as well as tables with the best model statistics, the LD/CV coefficient from the best model, and a summary of the iteration results. *Note 1*: if only two categories are used as group_column within a region, the results are displayed as histogram with superimposed density curves, otherwise, they are displayed with scatterplots and ellipses of confidence. *Note 2*: this hierarchical approach is outlined for two functional levels in the experimental sample. Should there be further levels, Step 11 can be repeated and adapted to extract the most often predicted classes from "Lev_n" and perform the LDA/cv-CVA on "Lev_{n+1}".

Establishing the most likely function of the archaeological tool entails assessing the results of the predictions. For both Steps 10 and 11, a table is produced with the predicted class and the probability the archaeological acquisition may belong to each class. The class

that consistently yields the highest probability may be interpreted as the most likely candidate to interpret the archaeological specimen from a quantitative surface texture perspective. Ideally, this result should converge with that reached with the qualitative use wear approach.

Supplementary Text S3. The *ExOsTechBank*

The *ExOsTechBank* database comprises 8,598 confocal acquisitions (as of 20 February 2025). These acquisitions are distributed as follow:

- 468 acquisitions of use-wear patterns present on ethnographic bone tools;
- 593 acquisitions of the natural surfaces of six species of herbivore long bone;
- 3,758 acquisitions of use-wear patterns present on experimental bone tools used in 44 activities including 20 activities involving plant processing, 13 hide working variants with and without abrasives, 5 soil digging activities and 4 animal butchery activities, etc.;
- 3,779 acquisitions of use-wear patterns and taphonomic alterations present on archaeological specimens found in 11 sites from Africa, East Asia and Europe.

The metadata for the acquisitions contains 43 fields to allow tracing the information on the institution where the sample is curated, the nature of the bone, the nature of the activity, whether the acquisition was done directly on the object or on elastomer imprints, the person who used the ethnographic or experimental tool, who made the acquisitions, etc. Access to the *ExOsTechBank* is available on request, however, any fields containing personal information will be anonymized prior to sharing the information.

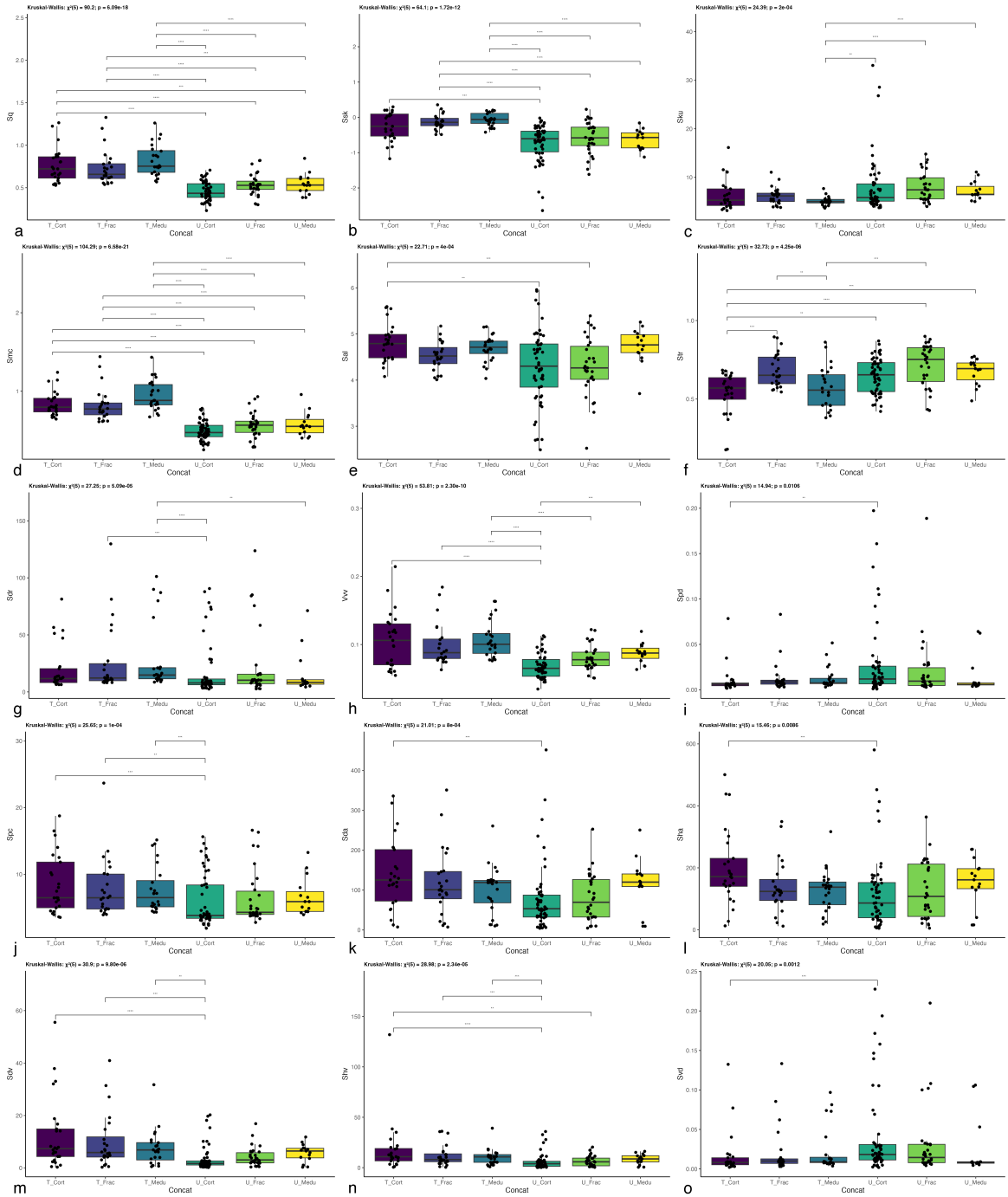

Figure S1.
Boxplots of the surface texture variables comparing worn (U) and unworn (T) areas on the cortical (Cort), medullar (Medu) and fracture plane (Frac) surfaces of the Abri du Maras specimen. *Sq* (a), *Ssk** (b), *Sku* (c), *Smc* (d), *Sal** (e), *Str** (f), *Sdr* (g), *Vvv* (h), *Spd** (i), *Spc* (j), *Sda* (k), *Sha* (l), *Sdv* (m), *Shv** (n), and *Svd* (o). See Table S1 for the definition of the surface texture parameters. Asterix above indicate surface texture variables that were identified as significant to distinguish worn and unworn surfaces and that were filtered for multivariate analysis after removing highly correlated variables.

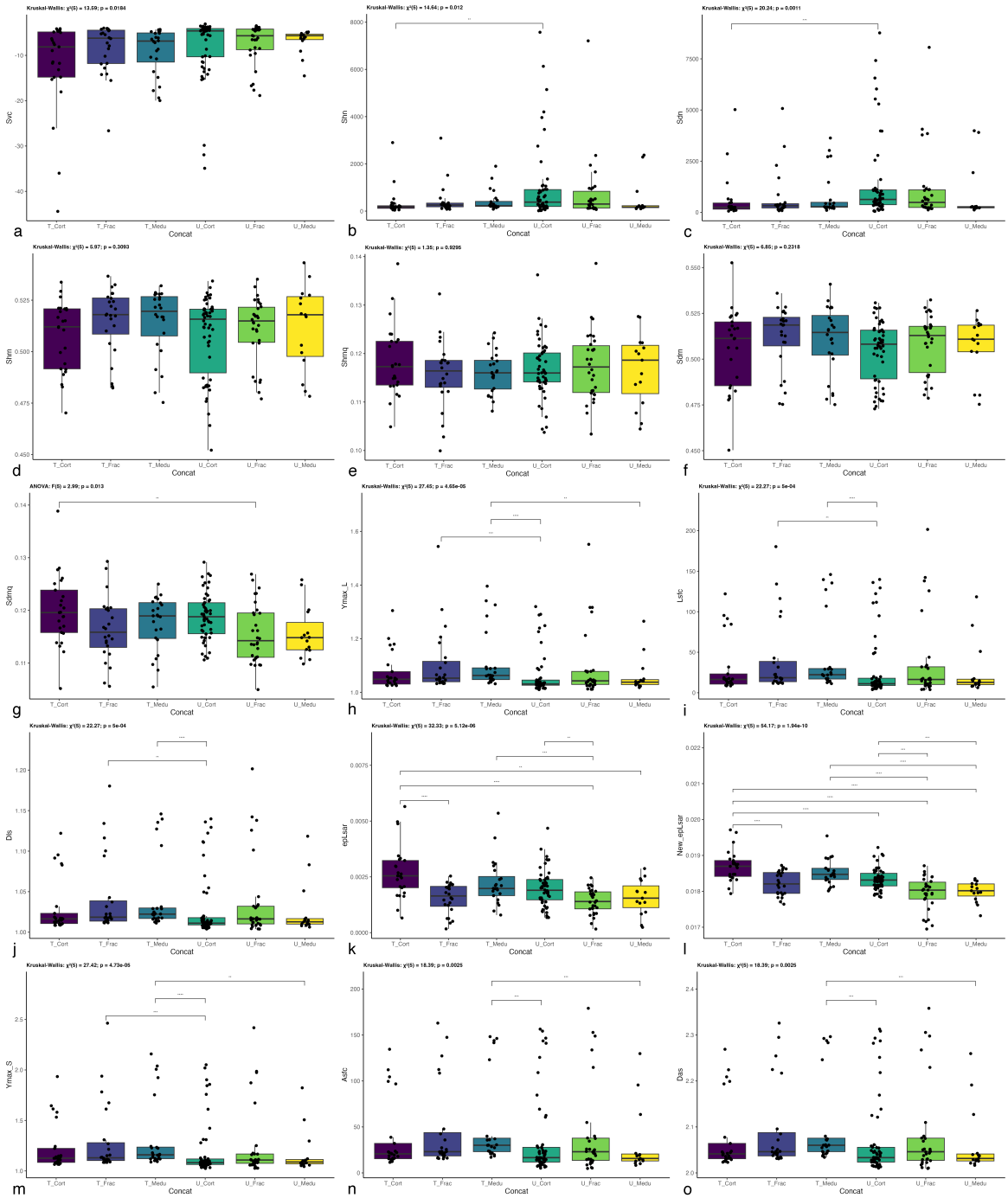

Figure S2.
Boxplots of the surface texture variables comparing worn (U) and unworn (T) areas on the cortical (Cort), medullar (Medu) and fracture plane (Frac) surfaces of the Abri du Maras specimen. *Svc* (a), *Shn* (b), *Sdn* (c), *Shrn* (d), *Shrnq* (e), *Sdrn* (f), *Sdrnq** (g), *Ymax_L* (h), *Lsfc* (i), *Dls* (j), *epLsar** (k), *New_epLsar* (l), *Ymax_S* (m), *Asfc* (n), and *Das* (o). See Table S1 for the definition of the surface texture parameters. Asterix above indicate surface texture variables that were identified as significant to distinguish worn and unworn surfaces and that were filtered for multivariate analysis after removing highly correlated variables.

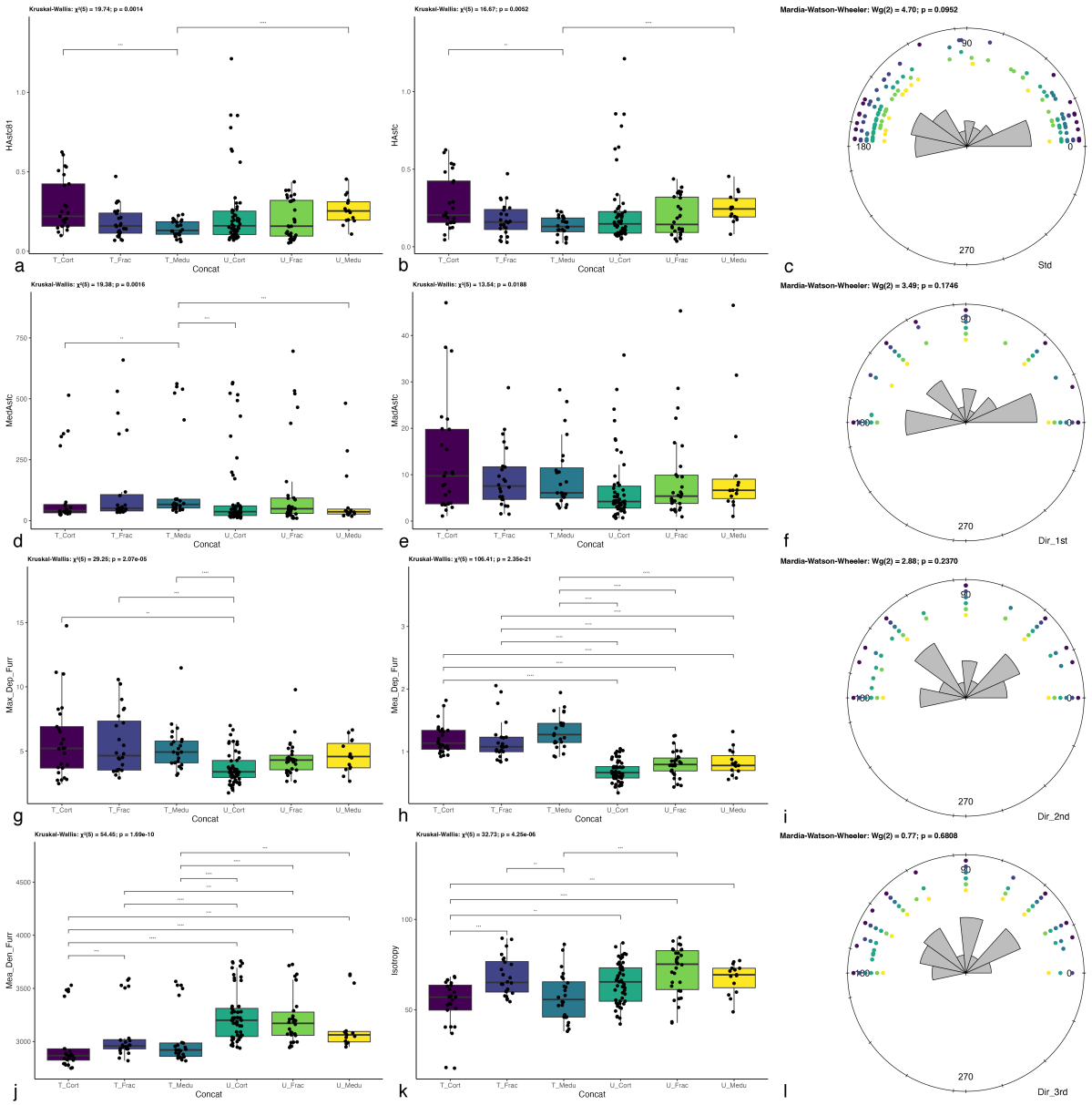

Figure S3.
Boxplots and rose diagrams of the surface texture variables comparing worn (U) and unworn (T) areas on the cortical (Cort), medullar (Medu) and fracture plane (Frac) surfaces of the Abri du Maras specimen. *HAsfc81** (a), *HAsfc* (b), *Std* (c), *Med_Asfc* (d), *Mad_Asfc** (e), *Dir_1st* (f), *Max_Dep_Furr* (g), *Mea_Dep_Furr** (h), *Dir_2nd* (i), *Mea_Den_Furr* (j), *Isotropy* (k), and *Dir_3rd* (l). See Table S1 for the definition of the surface texture parameters. Asterix above indicate surface texture variables that were identified as significant to distinguish worn and unworn surfaces and that were filtered for multivariate analysis after removing highly correlated variables.

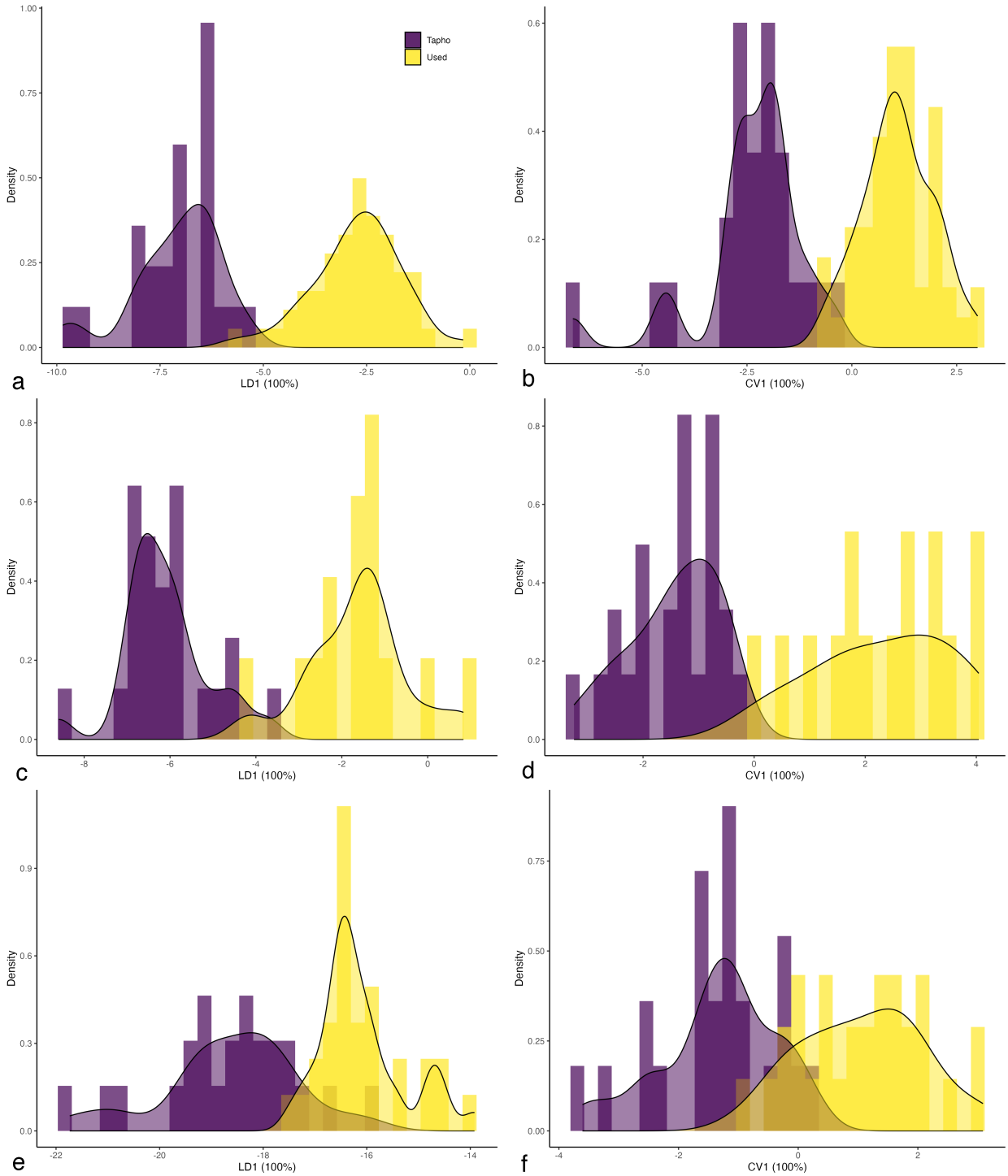

Figure S4.
Linear discriminant (LDA) (a, c, e) and cross-validation canonical variate (cv-CVA) (b, d, f) analyses results distinguishing worn (Used) and taphonomically altered (Tapho) areas on the cortical (a, b), medullar (c, d) and fracture plane (e, f) surfaces of the Abri du Maras specimen. See Tables S2-S7 for the corresponding confusion matrices and statistics.

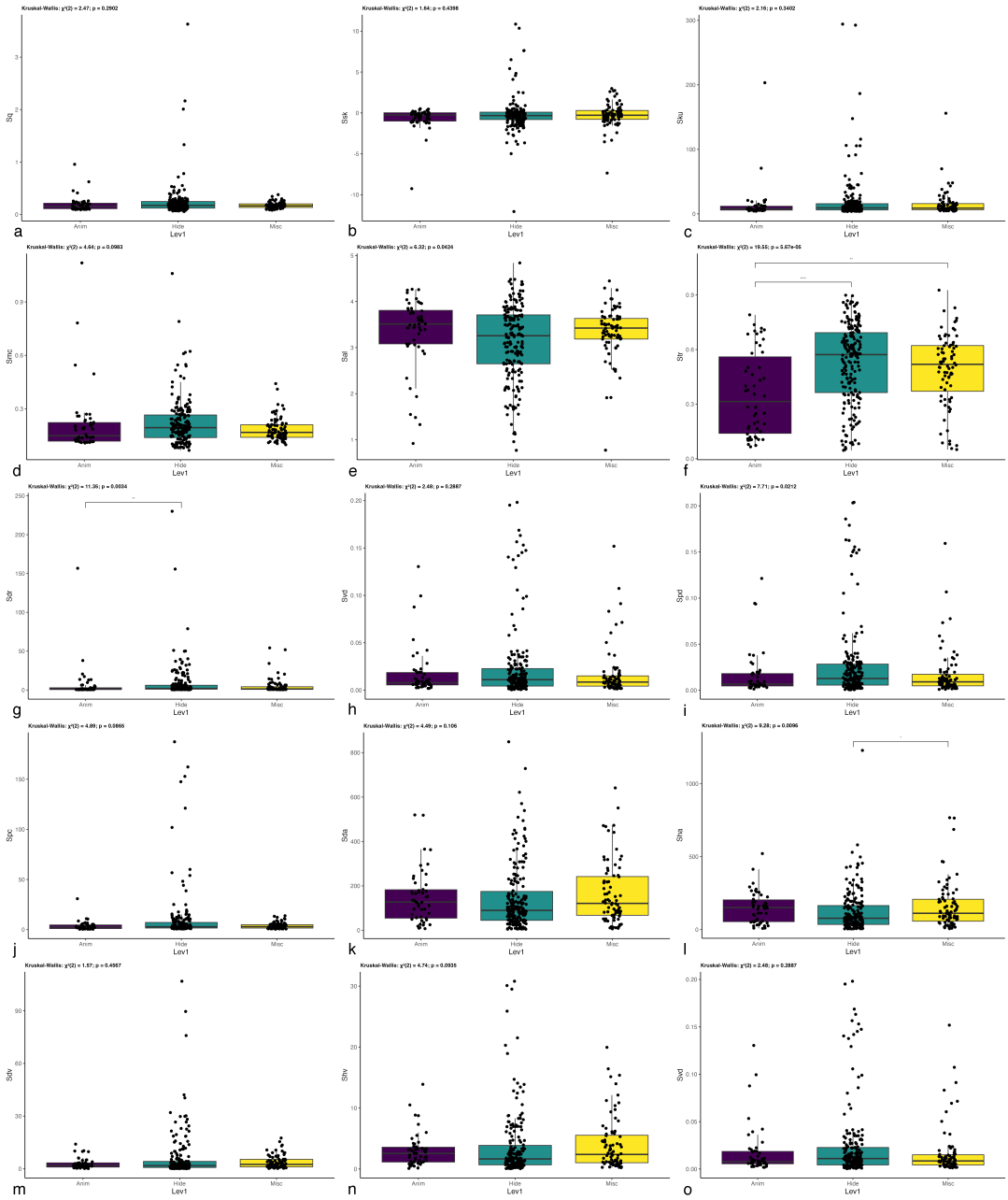

Figure S5.
Boxplots of the surface texture variables comparing broad categories of worked materials in the comparative experimental sample. Functional experiments included in the *Anim* category are flaying carcasses and cutting fresh meat. The *Hide* category encompasses rehydrated cow and deer hide without abrasive, dry hide with sand, fresh hide with sand, ochre, and marrow. The *Misc* category include debarking pine trees and digging in humic soil. *Sq* (a), *Ssk* (b), *Sku* (c), *Smc* (d), *Sal** (e), *Str** (f), *Sdr* (g), *Vvv* (h), *Spd* (i), *Spc* (j), *Sda* (k), *Sha** (l), *Sdv* (m), *Shv* (n), and *Svd* (o). See Table S1 for the definition of the surface texture parameters. Asterix above indicate surface texture variables that were identified as significant to distinguish the type of activity, and that were filtered for multivariate analysis after removing highly correlated variables.

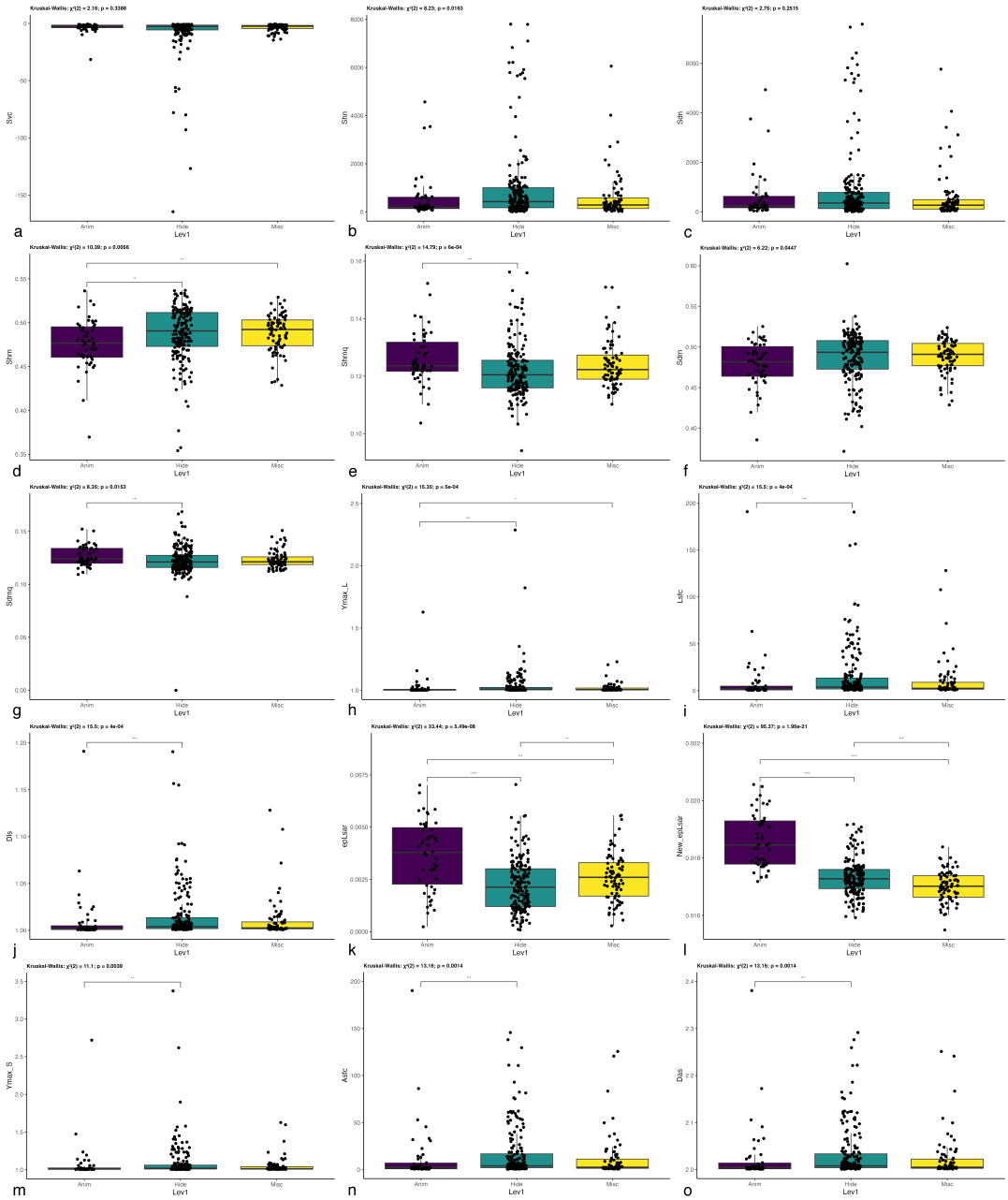

Figure S6.
Boxplots of the surface texture variables comparing broad categories of worked materials in the comparative experimental sample. Functional experiments included in the *Anim* category are flaying carcasses and cutting fresh meat. The *Hide* category encompasses rehydrated cow and deer hide without abrasive, dry hide with sand, fresh hide with sand, ochre, and marrow. The *Misc* category include debarking pine trees and digging in humic soil. *Svc* (a), *Shn** (b), *Sdn* (c), *Shrn** (d), *Shrnq** (e), *Sdrn* (f), *Sdrnq** (g), *Ymax_L** (h), *Lsfc* (i), *Dls* (j), *epLsar* (k), *New_epLsar** (l), *Ymax_S* (m), *Asfc* (n), and *Das* (o). See Table S1 for the definition of the surface texture parameters. Asterix above indicate surface texture variables that were identified as significant to distinguish the type of activity, and that were filtered for multivariate analysis after removing highly correlated variables.

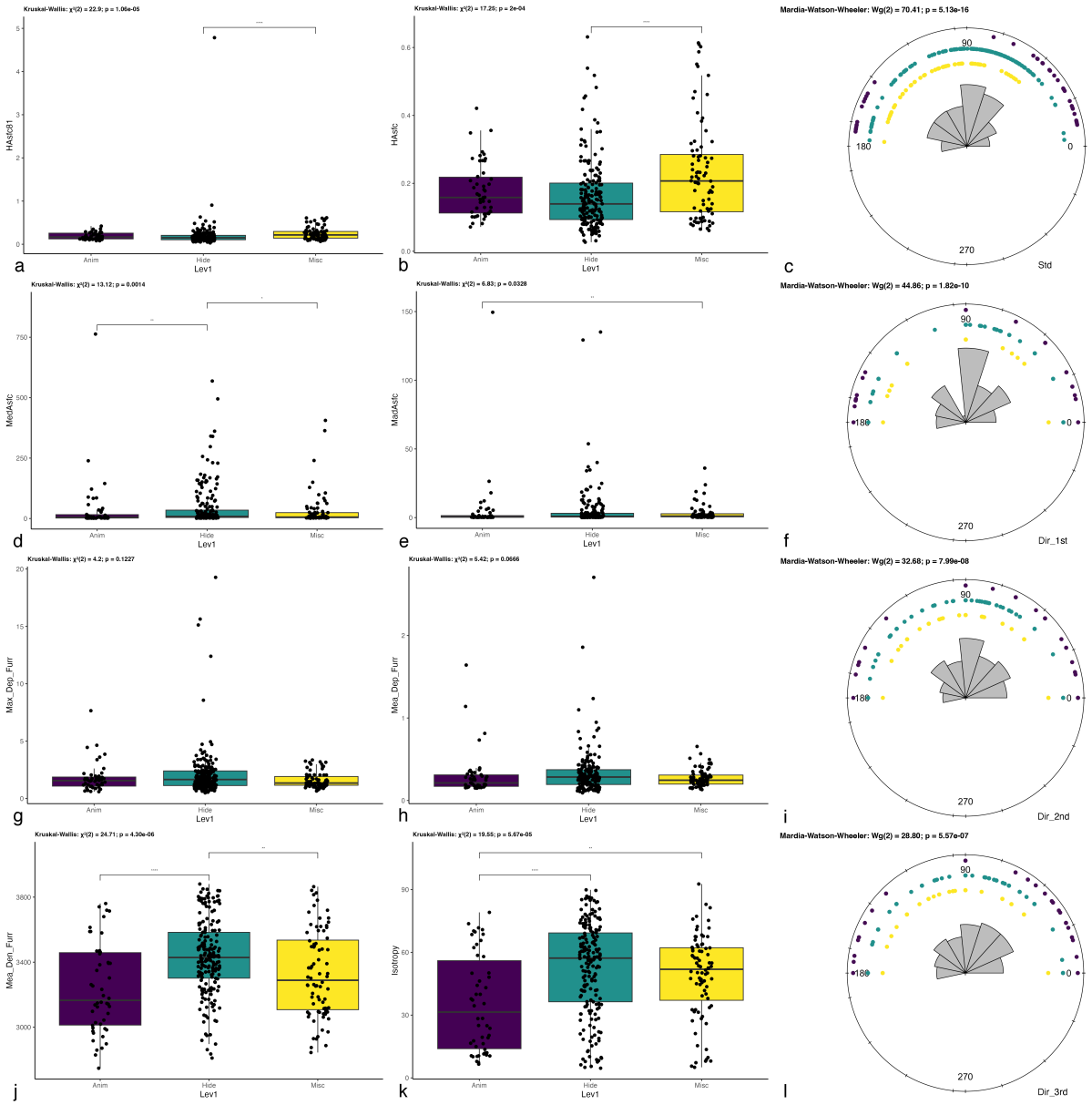

Figure S7.
Boxplots and rose diagrams of the surface texture variables comparing broad categories of worked materials in the comparative experimental sample. Functional experiments included in the *Anim* category are flaying carcasses and cutting fresh meat. The *Hide* category encompasses rehydrated cow and deer hide without abrasive, dry hide with sand, fresh hide with sand, ochre, and marrow. The *Misc* category include debarking pine trees and digging in humic soil. *HAsfc81** (a), *HAsfc** (b), *Std** (c), *Med_Asfc* (d), *Mad_Asfc* (e), *Dir_1st** (f), *Max_Dep_Furr* (g), *Mea_Dep_Furr* (h), *Dir_2nd** (i), *Mea_Den_Furr** (j), *Isotropy* (k), and *Dir_3rd** (l). See Table S1 for the definition of the surface texture parameters. Asterix above indicate surface texture variables that were identified as significant to distinguish the type of activity, and that were filtered for multivariate analysis after removing highly correlated variables.

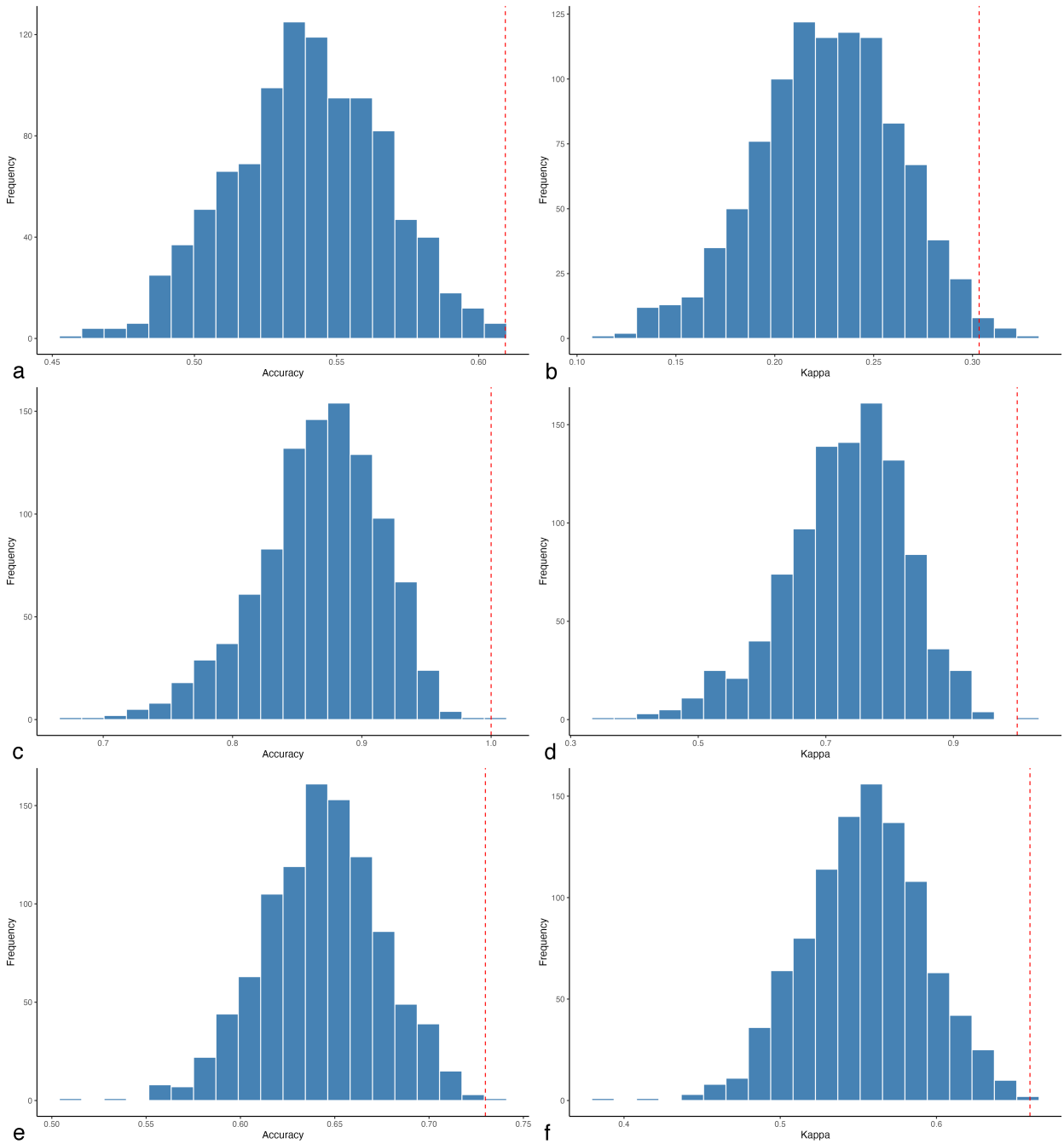

Figure S8.
Distribution of the overall accuracy (a, c, e) and kappa (b, d, f) statistics for the LDA across 1001 iterations. Accuracy and kappa statistics computed when discriminating general categories of worked material (a, b), i.e., animal soft tissues, hides, and bark or sediments, and when discriminating specific activities within the animal (c, d) or hide (e, f) categories. The red dash lines indicate the accuracy and kappa results for the best iteration that was used to predict the class on the Abri du Maras specimen.

Table S1.

Abbreviated codes, descriptions and units of the surface roughness parameters. "X" in the columns 'Step 3' and 'Step 7' indicates variables that were retained for the multivariate analyses in the present study, i.e., variables that yielded significant results in the pairwise comparisons and that were not highly correlated with others (see section "Data analysis" for more details).

Code	Description	Units	Step 3	Step 7
Sq	Root-mean-square height	µm		
Ssk	Skewness		X	
Sku	Kurtosis			
Smc	Inverse areal material ratio (10%)	µm		
Sal	Auto-correlation length (s = 0.2)	µm	X	X
Str *	Texture aspect ratio (s = 0.2)		X	X
Std **	Texture direction	°		X
Sdr *	Developed interfacial area ratio	%		
Vvv	Pit void volume (p = 80%)	$\mu m^3/\mu m^2$		
Spd	Density of peaks (pruning = 5%)	$1/\mu m^2$	X	
Spc	Arithmetic mean peak curvature (pruning = 5%)	1/µm		
Sda	Mean dale area (pruning = 5%)	μm^2		
Sha	Mean hill area (pruning = 5%)	μm^2		X
Sdv	Mean dale volume (pruning = 5%)	μm^3		
Shv	Mean hill volume (pruning = 5%)	μm^3	X	
Svd	Density of pits (pruning = 5%)	$1/\mu m^2$		
Svc	Arithmetic mean pit curvature (pruning = 5%)	1/µm		
Shn	Hill count			X
Sdn	Dale count			
Shrn	Mean hill roughness (pruning = 5%)			X
Shrnq	Standard deviation of hill roughness (pruning = 5%)			X
Sdrn	Mean dale roughness (pruning = 5%)			
Sdrnq	Standard deviation of dale roughness (pruning = 5%)		X	X
Ymax_L	Y-max (length-scale method)	- -		X
Lsfc	Fractal complexity (length-scale method)	- -		
Dls	Fractal dimension (length-scale method)	- -		
epLsar	Length-scale anisotropy (old)		X	
New_epLsar	Length-scale anisotropy (new)			X
Ymax_S	Y-max (area-scale method)			
Asfc	Fractal complexity (area-scale method)			
Das	Fractal dimension (area-scale method)			
HAsfc81	Heterogeneity of Asfc (9x9)		X	X
HAsfc	Heterogeneity of Asfc (3x3)			X
MedAsfc	Median of Asfc			
MadAsfc	Median absolute deviation of Asfc		X	
Max_Dep_Furr	Maximum depth of furrows	µm		
Mea_Dep_Furr	Mean depth of furrows	µm	X	
Mea_Den_Furr	Mean density of furrows	cm/cm^2		X
Isotropy *	Isotropy	%		
Dir_1st **	First direction of texture	°		X
Dir_2nd **	Second direction of texture	°		X
Dir_3rd **	Third direction of texture	°		X

* Note 1: prior to including this data in multivariate analyses, percentage and ratio values were transformed with the following formula: log(p/(1-p)) where p corresponds to the value expressed in percentage or ratio.

** Note 2: prior to including this data in multivariate analyses, angle values were transformed with the following formula: sin(radians(A˚)) +cos(radians(A˚)) where A˚ corresponds to the angle value expressed in degrees.

Table S2.

Confusion matrices for the LDA and cv-CVA discriminating between used and taphonomically altered areas on the cortical surface of the Abri du Maras specimen.

Class		LDA		cv-CVA	
		Actual			
		Tapho	Used	Tapho	Used
Predicted	Tapho	9	1	23	2
	Used	0	24	0	54

Table S3.

Overall and class statistics for the LDA and cv-CVA discriminating between used and taphonomically altered areas on the cortical surface of the Abri du Maras specimen.

		LDA	cv-CVA
Overall	Accuracy	97.06%	97.47%
	Kappa	92.70%	94.02%
	AccuracyLower	84.67%	91.15%
	AccuracyUpper	99.93%	99.69%
	AccuracyNull	73.53%	70.89%
	AccuracyPValue	0.04%	0.00%
	McnemarPValue	100.00%	47.95%
Class	Sensitivity	100.00%	100.00%
	Specificity	96.00%	96.43%
	Pos Pred Value	90.00%	92.00%
	Neg Pred Value	100.00%	100.00%
	Precision	90.00%	92.00%
	Recall	100.00%	100.00%
	F1	94.74%	95.83%
	Prevalence	26.47%	29.11%
	Detection Rate	26.47%	29.11%
	Detection Prevalence	29.41%	31.65%
	Balanced Accuracy	98.00%	98.21%

Table S4.

Confusion matrices for the LDA and cv-CVA discriminating between used and taphonomically altered areas on the medullar surface of the Abri du Maras specimen.

Class		LDA		cv-CVA	
		Actual			
		Tapho	Used	Tapho	Used
Predicted	Tapho	9	0	24	0
	Used	1	6	2	13

Table S5.

Overall and class statistics for the LDA and cv-CVA discriminating between used and taphonomically altered areas on the medullar surface of the Abri du Maras specimen.

		LDA	cv-CVA
Overall	Accuracy	93.75%	94.87%
	Kappa	87.10%	88.89%
	AccuracyLower	69.77%	82.68%
	AccuracyUpper	99.84%	99.37%
	AccuracyNull	62.50%	66.67%
	AccuracyPValue	0.57%	0.00%
	McnemarPValue	100.00%	47.95%
Class	Sensitivity	90.00%	92.31%
	Specificity	100.00%	100.00%
	Pos Pred Value	100.00%	100.00%
	Neg Pred Value	85.71%	86.67%
	Precision	100.00%	100.00%
	Recall	90.00%	92.31%
	F1	94.74%	96.00%
	Prevalence	62.50%	66.67%
	Detection Rate	56.25%	61.54%
	Detection Prevalence	56.25%	61.54%
	Balanced Accuracy	95.00%	96.15%

Table S6.

Confusion matrices for the LDA and cv-CVA discriminating between used and taphonomically altered areas on the fracture planes of the Abri du Maras specimen.

Class		LDA		cv-CVA	
		Actual			
		Tapho	Used	Tapho	Used
Predicted	Tapho	9	1	19	5
	Used	2	14	4	26

Table S7.

Overall and class statistics for the LDA and cv-CVA discriminating between used and taphonomically altered areas on the fracture planes of the Abri du Maras specimen.

		LDA	cv-CVA
Overall	Accuracy	88.46%	83.33%
	Kappa	76.07%	66.11%
	AccuracyLower	69.85%	70.71%
	AccuracyUpper	97.55%	92.08%
	AccuracyNull	57.69%	57.41%
	AccuracyPValue	0.08%	0.00%
	McnemarPValue	100.00%	100.00%
Class	Sensitivity	81.82%	82.61%
	Specificity	93.33%	83.87%
	Pos Pred Value	90.00%	79.17%
	Neg Pred Value	87.50%	86.67%
	Precision	90.00%	79.17%
	Recall	81.82%	82.61%
	F1	85.71%	80.85%
	Prevalence	42.31%	42.59%
	Detection Rate	34.62%	35.19%
	Detection Prevalence	38.46%	44.44%
	Balanced Accuracy	87.58%	83.24%

Table S8.

LDA and cv-CVA predictions for the broad categories of material that likely came into contact with the Abri du Maras specimen.

	LDA (Level 1)				cv-CVA (Level 1)			
Acquisition ID	Prediction	Prob. Anim	Prob. Hide	Prob. Misc	Prediction	Prob. Anim	Prob. Hide	Prob. Misc
Maras_2017_W10_1_A	Hide	25.51%	47.25%	27.24%	Hide	6.67%	73.33%	20.00%
Maras_2017_W11_1_A	Hide	22.67%	67.29%	10.05%	Misc	13.33%	40.00%	46.67%
Maras_2017_W12_1_A	Misc	31.71%	12.93%	55.36%	Misc	13.33%	40.00%	46.67%
Maras_2017_W13_1_A	Anim	96.53%	1.35%	2.12%	Hide	13.33%	46.67%	40.00%
Maras_2017_W14_1_A	Hide	33.82%	40.01%	26.18%	Hide	0.00%	66.67%	33.33%
Maras_2017_W17_1_A	Misc	0.01%	24.73%	75.26%	Hide	6.67%	73.33%	20.00%
Maras_2017_W18_1_A	Hide	1.64%	50.40%	47.96%	Hide	13.33%	53.33%	33.33%
Maras_2017_W19_1_A	Hide	0.48%	96.46%	3.06%	Hide	0.00%	73.33%	26.67%
Maras_2017_W20_1_A	Hide	9.17%	73.75%	17.08%	Hide	0.00%	53.33%	46.67%
Maras_2017_W10_1_B	Hide	0.43%	53.55%	46.02%	Hide	20.00%	53.33%	26.67%
Maras_2017_W11_1_B	Anim	78.86%	16.87%	4.27%	Hide	0.00%	66.67%	33.33%
Maras_2017_W12_1_B	Hide	14.84%	71.68%	13.48%	Hide	6.67%	66.67%	26.67%
Maras_2017_W14_1_B	Misc	0.23%	26.05%	73.73%	Hide	0.00%	73.33%	26.67%
Maras_2017_W15_1_B	Anim	96.41%	1.25%	2.34%	Hide	0.00%	66.67%	33.33%
Maras_2017_W16_1_B	Hide	46.04%	48.91%	5.05%	Misc	13.33%	40.00%	46.67%
Maras_2017_W17_1_B	Hide	38.48%	59.46%	2.06%	Hide	6.67%	60.00%	33.33%
Maras_2017_W18_1_B	Misc	0.26%	1.59%	98.15%	Misc	0.00%	26.67%	73.33%
Maras_2017_W19_1_B	Anim	92.81%	4.46%	2.73%	Misc	13.33%	40.00%	46.67%
Maras_2017_W20_1_B	Anim	99.79%	0.11%	0.10%	Hide	0.00%	60.00%	40.00%
Maras_2017_W10_1_C	Hide	1.17%	64.98%	33.84%	Hide	0.00%	66.67%	33.33%
Maras_2017_W11_1_C	Hide	5.09%	93.67%	1.24%	Hide	13.33%	53.33%	33.33%
Maras_2017_W12_1_C	Hide	7.68%	91.52%	0.80%	Misc	6.67%	40.00%	53.33%
Maras_2017_W13_1_C	Anim	92.42%	7.15%	0.44%	Hide	0.00%	73.33%	26.67%
Maras_2017_W14_1_C	Hide	42.78%	50.70%	6.52%	Hide	0.00%	53.33%	46.67%
Maras_2017_W15_1_C	Hide	0.60%	66.90%	32.50%	Misc	0.00%	46.67%	53.33%
Maras_2017_W16_1_C	Anim	68.13%	28.59%	3.28%	Misc	0.00%	46.67%	53.33%
Maras_2017_W17_1_C	Hide	11.82%	64.73%	23.46%	Misc	13.33%	40.00%	46.67%
Maras_2017_W18_1_C	Anim	91.41%	4.15%	4.44%	Hide	13.33%	53.33%	33.33%
Maras_2017_W19_1_C	Hide	33.12%	66.06%	0.82%	Misc	0.00%	26.67%	73.33%
Maras_2017_W20_1_C	Hide	3.26%	67.07%	29.67%	Hide	0.00%	60.00%	40.00%
Maras_2017_W10_1_D	Hide	0.30%	93.23%	6.48%	Misc	13.33%	33.33%	53.33%
Maras_2017_W11_1_D	Misc	28.92%	1.61%	69.47%	Misc	13.33%	40.00%	46.67%
Maras_2017_W12_1_D	Anim	59.90%	36.87%	3.23%	Hide	0.00%	73.33%	26.67%
Maras_2017_W13_1_D	Misc	21.75%	3.18%	75.07%	Misc	13.33%	40.00%	46.67%
Maras_2017_W14_1_D	Anim	65.32%	20.63%	14.05%	Hide	6.67%	66.67%	26.67%
Maras_2017_W15_1_D	Anim	84.54%	13.27%	2.18%	Misc	13.33%	40.00%	46.67%
Maras_2017_W16_1_D	Hide	5.96%	75.14%	18.90%	Misc	13.33%	40.00%	46.67%
Maras_2017_W17_1_D	Hide	31.10%	63.36%	5.53%	Misc	6.67%	40.00%	53.33%
Maras_2017_W19_1_D	Hide	1.16%	97.96%	0.87%	Hide	0.00%	53.33%	46.67%
Maras_2017_W20_1_D	Anim	98.47%	0.68%	0.84%	Hide	0.00%	53.33%	46.67%
Maras_2017_W10_1_E	Hide	11.33%	46.04%	42.63%	Hide	6.67%	73.33%	20.00%
Maras_2017_W11_1_E	Anim	98.47%	1.20%	0.33%	Misc	0.00%	40.00%	60.00%
Maras_2017_W12_1_E	Hide	0.74%	66.46%	32.80%	Hide	0.00%	66.67%	33.33%
Maras_2017_W13_1_E	Anim	74.96%	6.57%	18.47%	Hide	13.33%	46.67%	40.00%
Maras_2017_W14_1_E	Hide	0.41%	70.32%	29.28%	Misc	13.33%	33.33%	53.33%
Maras_2017_W15_1_E	Anim	62.25%	20.84%	16.90%	Hide	20.00%	60.00%	20.00%
Maras_2017_W16_1_E	Anim	97.45%	1.93%	0.63%	Hide	13.33%	53.33%	33.33%
Maras_2017_W17_1_E	Hide	0.01%	97.56%	2.43%	Hide	0.00%	66.67%	33.33%
Maras_2017_W19_1_E	Hide	0.05%	99.03%	0.92%	Misc	6.67%	40.00%	53.33%
Maras_2017_W20_1_E	Hide	1.83%	82.30%	15.87%	Misc	0.00%	46.67%	53.33%

Table S9.

LDA and cv-CVA predictions for the activities involving hide that could explain the use wear pattern on the Abri du Maras specimen. The high number of differences in predictions between the LDA and the cv-CVA suggests it is unlikely the Abri du Maras tool was used to process hides.

	LDA (Hide)							cv-CVA (Hide)						
Acquisition ID	Prediction	Dry hide with sand	Fresh hide with marrow	Fresh hide with ochre	Fresh hide with sand	Rehydrated hide - Bovid	Rehydrated hide - Cervid	Prediction	Dry hide with sand	Fresh hide with marrow	Fresh hide with ochre	Fresh hide with sand	Rehydrated hide - Bovid	Rehydrated hide - Cervid
Maras_2017_W10_1_A	DrySand	100.00%	0.00%	0.00%	0.00%	0.00%	0.00%	FreMarr	7.14%	64.29%	21.43%	0.00%	7.14%	0.00%
Maras_2017_W11_1_A	DrySand	100.00%	0.00%	0.00%	0.00%	0.00%	0.00%	FreOchr	7.14%	42.86%	50.00%	0.00%	0.00%	0.00%
Maras_2017_W12_1_A	DrySand	100.00%	0.00%	0.00%	0.00%	0.00%	0.00%	FreOchr	0.00%	50.00%	50.00%	0.00%	0.00%	0.00%
Maras_2017_W13_1_A	RehNoAbr_C	0.00%	0.00%	0.00%	0.00%	0.00%	99.99%	FreMarr	0.00%	64.29%	35.71%	0.00%	0.00%	0.00%
Maras_2017_W14_1_A	DrySand	100.00%	0.00%	0.00%	0.00%	0.00%	0.00%	FreMarr	42.86%	42.86%	14.29%	0.00%	0.00%	0.00%
Maras_2017_W17_1_A	DrySand	99.82%	0.04%	0.14%	0.00%	0.00%	0.00%	FreMarr	7.14%	57.14%	28.57%	0.00%	0.00%	7.14%
Maras_2017_W18_1_A	DrySand	99.73%	0.00%	0.00%	0.00%	0.00%	0.26%	FreMarr	14.29%	35.71%	14.29%	14.29%	0.00%	21.43%
Maras_2017_W19_1_A	DrySand	100.00%	0.00%	0.00%	0.00%	0.00%	0.00%	DrySand	50.00%	35.71%	14.29%	0.00%	0.00%	0.00%
Maras_2017_W20_1_A	DrySand	100.00%	0.00%	0.00%	0.00%	0.00%	0.00%	FreOchr	14.29%	42.86%	42.86%	0.00%	0.00%	0.00%
Maras_2017_W10_1_B	DrySand	85.69%	11.00%	3.31%	0.00%	0.00%	0.00%	FreMarr	35.71%	42.86%	7.14%	0.00%	0.00%	14.29%
Maras_2017_W11_1_B	DrySand	99.83%	0.00%	0.11%	0.05%	0.00%	0.01%	FreOchr	0.00%	35.71%	64.29%	0.00%	0.00%	0.00%
Maras_2017_W12_1_B	DrySand	100.00%	0.00%	0.00%	0.00%	0.00%	0.00%	DrySand	57.14%	28.57%	14.29%	0.00%	0.00%	0.00%
Maras_2017_W14_1_B	DrySand	44.28%	42.53%	13.19%	0.00%	0.00%	0.00%	DrySand	42.86%	42.86%	14.29%	0.00%	0.00%	0.00%
Maras_2017_W15_1_B	DrySand	100.00%	0.00%	0.00%	0.00%	0.00%	0.00%	FreOchr	0.00%	35.71%	57.14%	0.00%	0.00%	7.14%
Maras_2017_W16_1_B	DrySand	100.00%	0.00%	0.00%	0.00%	0.00%	0.00%	FreOchr	28.57%	28.57%	42.86%	0.00%	0.00%	0.00%
Maras_2017_W17_1_B	DrySand	99.92%	0.00%	0.02%	0.06%	0.00%	0.00%	FreSand	0.00%	14.29%	28.57%	28.57%	7.14%	21.43%
Maras_2017_W18_1_B	RehNoAbr_C	0.05%	0.47%	0.04%	0.00%	0.00%	99.44%	FreSand	7.14%	21.43%	21.43%	28.57%	0.00%	21.43%
Maras_2017_W19_1_B	DrySand	100.00%	0.00%	0.00%	0.00%	0.00%	0.00%	FreOchr	14.29%	35.71%	50.00%	0.00%	0.00%	0.00%
Maras_2017_W20_1_B	DrySand	100.00%	0.00%	0.00%	0.00%	0.00%	0.00%	RehNoAbr_C	7.14%	14.29%	14.29%	7.14%	0.00%	57.14%
Maras_2017_W10_1_C	DrySand	95.31%	1.23%	3.47%	0.00%	0.00%	0.00%	FreMarr	0.00%	57.14%	35.71%	0.00%	0.00%	7.14%
Maras_2017_W11_1_C	DrySand	100.00%	0.00%	0.00%	0.00%	0.00%	0.00%	FreMarr	7.14%	50.00%	42.86%	0.00%	0.00%	0.00%
Maras_2017_W12_1_C	DrySand	100.00%	0.00%	0.00%	0.00%	0.00%	0.00%	FreMarr	21.43%	57.14%	21.43%	0.00%	0.00%	0.00%
Maras_2017_W13_1_C	DrySand	100.00%	0.00%	0.00%	0.00%	0.00%	0.00%	DrySand	42.86%	35.71%	21.43%	0.00%	0.00%	0.00%
Maras_2017_W14_1_C	DrySand	100.00%	0.00%	0.00%	0.00%	0.00%	0.00%	DrySand	42.86%	35.71%	21.43%	0.00%	0.00%	0.00%
Maras_2017_W15_1_C	DrySand	99.90%	0.08%	0.02%	0.00%	0.00%	0.00%	DrySand	42.86%	35.71%	21.43%	0.00%	0.00%	0.00%
Maras_2017_W16_1_C	DrySand	99.56%	0.00%	0.28%	0.16%	0.00%	0.00%	DrySand	57.14%	28.57%	14.29%	0.00%	0.00%	0.00%
Maras_2017_W17_1_C	DrySand	99.99%	0.00%	0.00%	0.00%	0.00%	0.00%	FreMarr	14.29%	42.86%	21.43%	7.14%	7.14%	7.14%
Maras_2017_W18_1_C	DrySand	99.99%	0.00%	0.00%	0.00%	0.00%	0.00%	FreOchr	0.00%	42.86%	57.14%	0.00%	0.00%	0.00%
Maras_2017_W19_1_C	DrySand	99.94%	0.00%	0.01%	0.05%	0.00%	0.00%	DrySand	50.00%	35.71%	14.29%	0.00%	0.00%	0.00%
Maras_2017_W20_1_C	DrySand	97.33%	2.64%	0.03%	0.00%	0.00%	0.00%	FreMarr	21.43%	42.86%	28.57%	0.00%	0.00%	7.14%
Maras_2017_W10_1_D	DrySand	84.27%	5.15%	10.27%	0.31%	0.00%	0.00%	FreMarr	28.57%	42.86%	28.57%	0.00%	0.00%	0.00%
Maras_2017_W11_1_D	FreMarr	2.30%	93.99%	3.34%	0.00%	0.00%	0.37%	FreMarr	35.71%	50.00%	14.29%	0.00%	0.00%	0.00%
Maras_2017_W12_1_D	DrySand	99.38%	0.00%	0.55%	0.06%	0.00%	0.00%	FreOchr	21.43%	35.71%	42.86%	0.00%	0.00%	0.00%
Maras_2017_W13_1_D	DrySand	100.00%	0.00%	0.00%	0.00%	0.00%	0.00%	FreMarr	0.00%	57.14%	28.57%	7.14%	0.00%	7.14%
Maras_2017_W14_1_D	DrySand	99.97%	0.03%	0.00%	0.00%	0.00%	0.00%	DrySand	71.43%	21.43%	7.14%	0.00%	0.00%	0.00%
Maras_2017_W15_1_D	DrySand	84.00%	0.02%	4.40%	11.58%	0.00%	0.00%	FreMarr	0.00%	57.14%	28.57%	7.14%	0.00%	7.14%
Maras_2017_W16_1_D	DrySand	96.58%	3.41%	0.01%	0.00%	0.00%	0.00%	FreMarr	0.00%	57.14%	42.86%	0.00%	0.00%	0.00%
Maras_2017_W17_1_D	DrySand	96.28%	0.12%	2.51%	1.10%	0.00%	0.00%	FreMarr	14.29%	57.14%	28.57%	0.00%	0.00%	0.00%
Maras_2017_W19_1_D	DrySand	99.99%	0.00%	0.00%	0.00%	0.00%	0.00%	FreOchr	14.29%	42.86%	42.86%	0.00%	0.00%	0.00%
Maras_2017_W20_1_D	DrySand	100.00%	0.00%	0.00%	0.00%	0.00%	0.00%	RehNoAbr_C	7.14%	14.29%	14.29%	7.14%	0.00%	57.14%
Maras_2017_W10_1_E	DrySand	96.32%	2.84%	0.84%	0.00%	0.00%	0.00%	FreMarr	0.00%	57.14%	7.14%	0.00%	28.57%	7.14%
Maras_2017_W11_1_E	DrySand	99.99%	0.00%	0.00%	0.01%	0.00%	0.00%	FreMarr	14.29%	57.14%	28.57%	0.00%	0.00%	0.00%
Maras_2017_W12_1_E	DrySand	99.94%	0.06%	0.00%	0.00%	0.00%	0.00%	FreOchr	0.00%	35.71%	42.86%	14.29%	0.00%	7.14%
Maras_2017_W13_1_E	DrySand	85.70%	0.00%	0.00%	0.00%	0.00%	14.29%	FreMarr	21.43%	57.14%	14.29%	0.00%	0.00%	7.14%
Maras_2017_W14_1_E	DrySand	99.99%	0.01%	0.00%	0.00%	0.00%	0.00%	FreMarr	28.57%	57.14%	14.29%	0.00%	0.00%	0.00%
Maras_2017_W15_1_E	DrySand	100.00%	0.00%	0.00%	0.00%	0.00%	0.00%	DrySand	64.29%	35.71%	0.00%	0.00%	0.00%	0.00%
Maras_2017_W16_1_E	DrySand	99.99%	0.01%	0.00%	0.00%	0.00%	0.00%	DrySand	57.14%	42.86%	0.00%	0.00%	0.00%	0.00%
Maras_2017_W17_1_E	FreOchr	42.62%	11.91%	44.84%	0.63%	0.00%	0.01%	DrySand	78.57%	7.14%	14.29%	0.00%	0.00%	0.00%
Maras_2017_W19_1_E	DrySand	99.94%	0.01%	0.06%	0.00%	0.00%	0.00%	DrySand	57.14%	28.57%	14.29%	0.00%	0.00%	0.00%
Maras_2017_W20_1_E	DrySand	99.99%	0.01%	0.00%	0.00%	0.00%	0.00%	DrySand	71.43%	14.29%	14.29%	0.00%	0.00%	0.00%

Table S10.

LDA and cv-CVA predictions for the activities involving soft animal tissues other than hide that could explain the use wear pattern on the Abri du Maras specimen. The high number of similitudes in predictions between the LDA and the cv-CVA suggests it is likely the Abri du Maras tool was used to flaying carcasses.

	LDA (Anim)			cv-CVA (Anim)		
Acquisition ID	Prediction	Flaying carcass	Cutting fresh meat	Prediction	Flaying carcass	Cutting fresh meat
Maras_2017_W10_1_A	Flaying	100.00%	0.00%	Flaying	100.00%	0.00%
Maras_2017_W11_1_A	Flaying	99.98%	0.02%	Flaying	100.00%	0.00%
Maras_2017_W12_1_A	Flaying	100.00%	0.00%	Flaying	100.00%	0.00%
Maras_2017_W13_1_A	Flaying	100.00%	0.00%	Flaying	100.00%	0.00%
Maras_2017_W14_1_A	Flaying	100.00%	0.00%	Flaying	100.00%	0.00%
Maras_2017_W17_1_A	Flaying	100.00%	0.00%	Flaying	100.00%	0.00%
Maras_2017_W18_1_A	Flaying	100.00%	0.00%	Flaying	100.00%	0.00%
Maras_2017_W19_1_A	Flaying	100.00%	0.00%	Flaying	100.00%	0.00%
Maras_2017_W20_1_A	FreMeat	0.40%	99.60%	Flaying	100.00%	0.00%
Maras_2017_W10_1_B	Flaying	96.31%	3.69%	Flaying	100.00%	0.00%
Maras_2017_W11_1_B	Flaying	100.00%	0.00%	Flaying	100.00%	0.00%
Maras_2017_W12_1_B	Flaying	68.05%	31.95%	Flaying	100.00%	0.00%
Maras_2017_W14_1_B	Flaying	100.00%	0.00%	Flaying	100.00%	0.00%
Maras_2017_W15_1_B	Flaying	100.00%	0.00%	Flaying	100.00%	0.00%
Maras_2017_W16_1_B	FreMeat	0.05%	99.95%	Flaying	100.00%	0.00%
Maras_2017_W17_1_B	Flaying	100.00%	0.00%	Flaying	100.00%	0.00%
Maras_2017_W18_1_B	Flaying	100.00%	0.00%	Flaying	100.00%	0.00%
Maras_2017_W19_1_B	Flaying	100.00%	0.00%	Flaying	100.00%	0.00%
Maras_2017_W20_1_B	Flaying	82.02%	17.98%	Flaying	100.00%	0.00%
Maras_2017_W10_1_C	Flaying	84.42%	15.58%	Flaying	100.00%	0.00%
Maras_2017_W11_1_C	FreMeat	0.07%	99.93%	Flaying	100.00%	0.00%
Maras_2017_W12_1_C	FreMeat	45.47%	54.53%	Flaying	100.00%	0.00%
Maras_2017_W13_1_C	Flaying	100.00%	0.00%	Flaying	100.00%	0.00%
Maras_2017_W14_1_C	Flaying	97.87%	2.13%	Flaying	100.00%	0.00%
Maras_2017_W15_1_C	FreMeat	0.26%	99.74%	Flaying	100.00%	0.00%
Maras_2017_W16_1_C	FreMeat	0.96%	99.04%	Flaying	100.00%	0.00%
Maras_2017_W17_1_C	Flaying	99.46%	0.54%	Flaying	100.00%	0.00%
Maras_2017_W18_1_C	Flaying	100.00%	0.00%	Flaying	100.00%	0.00%
Maras_2017_W19_1_C	Flaying	99.98%	0.02%	Flaying	100.00%	0.00%
Maras_2017_W20_1_C	FreMeat	0.00%	100.00%	Flaying	100.00%	0.00%
Maras_2017_W10_1_D	Flaying	58.54%	41.46%	Flaying	100.00%	0.00%
Maras_2017_W11_1_D	Flaying	100.00%	0.00%	Flaying	100.00%	0.00%
Maras_2017_W12_1_D	Flaying	100.00%	0.00%	Flaying	71.43%	28.57%
Maras_2017_W13_1_D	Flaying	100.00%	0.00%	Flaying	100.00%	0.00%
Maras_2017_W14_1_D	Flaying	100.00%	0.00%	Flaying	100.00%	0.00%
Maras_2017_W15_1_D	Flaying	100.00%	0.00%	Flaying	100.00%	0.00%
Maras_2017_W16_1_D	FreMeat	10.39%	89.61%	Flaying	100.00%	0.00%
Maras_2017_W17_1_D	Flaying	100.00%	0.00%	Flaying	100.00%	0.00%
Maras_2017_W19_1_D	Flaying	96.41%	3.59%	Flaying	100.00%	0.00%
Maras_2017_W20_1_D	FreMeat	0.01%	99.99%	Flaying	100.00%	0.00%
Maras_2017_W10_1_E	Flaying	99.86%	0.14%	FreMeat	42.86%	57.14%
Maras_2017_W11_1_E	Flaying	99.97%	0.03%	Flaying	100.00%	0.00%
Maras_2017_W12_1_E	Flaying	99.19%	0.81%	Flaying	100.00%	0.00%
Maras_2017_W13_1_E	Flaying	100.00%	0.00%	Flaying	100.00%	0.00%
Maras_2017_W14_1_E	Flaying	100.00%	0.00%	Flaying	100.00%	0.00%
Maras_2017_W15_1_E	Flaying	99.97%	0.03%	FreMeat	0.00%	100.00%
Maras_2017_W16_1_E	Flaying	82.30%	17.70%	Flaying	85.71%	14.29%
Maras_2017_W17_1_E	Flaying	99.96%	0.04%	Flaying	71.43%	28.57%
Maras_2017_W19_1_E	FreMeat	12.96%	87.04%	Flaying	100.00%	0.00%
Maras_2017_W20_1_E	FreMeat	0.00%	100.00%	Flaying	71.43%	28.57%

Supplementary Data S1. (separate file)

Surface texture data acquired on the comparative experimental sample and on the abri du Maras specimen. Confocal acquisitions obtained on the abri du Maras specimen are available online (Zenedo: 10.5281/zenodo.15630707) alongside the R code used for this study. Access to the comparative experimental sample selected from the *ExOsTechBank* may be granted upon request to the corresponding author.